ACS OMEGA

http://pubs.acs.org/journal/acsodf

Article

CFD Simulation of the Airborne Transmission of COVID-19 Vectors Emitted during Respiratory Mechanisms: Revisiting the Concept of Safe Distance

Mariam, Ashish Magar, Manish Joshi, Pachalla S. Rajagopal, Arshad Khan, Madhukar M. Rao, and Balvinder K. Sapra*

Cite This: *ACS Omega* 2021, 6, 16876−16889

Read Online

ACCESS | Metrics & More | Article Recommendations | Supporting Information

ABSTRACT: The airborne transmission of the COVID-19 virus has been suggested as a major mode of transmission in recent studies. In this context, we studied the spatial transmission of COVID-19 vectors in an indoor setting representative of a typical office room. Computational fluid dynamics (CFD) simulations were performed to study the airborne dispersion of particles ejected due to different respiratory mechanisms, i.e., coughing, sneezing, normal talking, and loud talking. Number concentration profiles at a distance of 2 m in front of the emitter at the ventilation rates of 4, 6, and 8 air changes per hour (ACH) were estimated for different combinations of inlet−outlet positions and emitter−receptor configurations. Apart from respiratory events, viz., coughing and sneezing characterized by higher velocity and concentration of ejected particles, normal as well as loud talking was seen to be carrying particles to the receptor for some airflow patterns in the room. This study indicates that the ″rule of thumb based safe distance approach″ cannot be a general mitigation strategy for infection control. Under some scenarios, events with a lower release rate of droplets such as talking (i.e., asymptomatic transmission) can lead to a high concentration of particles persisting for long times. For better removal, the study suggests ″air curtains″ as an appropriate approach, simultaneously highlighting the pitfalls in the ″higher ventilation rate for better removal″ strategy. The inferences for talking-induced particle transmissions are crucial considering that large populations of COVID-19-infected persons are projected to be asymptomatic transmitters.

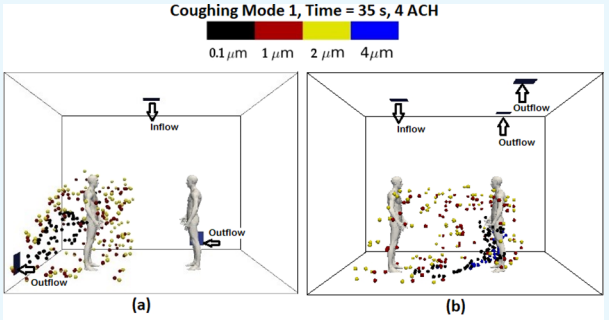

Role of inlet-outlet configuration in an enclosed space
(a) air curtain effect (b) breaching safe distance of 2 m

1. INTRODUCTION

The COVID-19 pandemic caused by the novel coronavirus SARS-COV-2 has changed the dynamics of the entire world, resulting in the loss of lives and collapsing economies. The severity of the ongoing second wave in countries, including India, has again prompted governments to plan an immediate recovery plan such as lockdowns, financial aid, and mass vaccination. Simultaneously, researchers across the world are focusing on long-term viable solutions including the ″future mitigation strategies″. The term ″Safe distance″ (2 m as per CDC[1] and NHS;[2] 1 m as per WHO[3]) is coined on the basis of fall-out of respiratory droplets (ejected via sneezing or coughing), one of the modes of transmission of the coronavirus.[4] On the basis of several studies[5−7] conducted worldwide, the debate of ″transmission through the airborne route″ seems to be settling with listed and corroborated scientific evidences.[8] Although reasonable for large droplet-based transmission, the concept of safe distance seems shaky if the virus transmits as/through aerosol particles. Even the 5 μm particle size threshold, which is used to differentiate droplets (>5 μm) from aerosol particles (<5 μm),[9,10] may require recalibrations for different contexts involving complicated size-varying aerosol transport and deposition.

Four main mechanistic processes responsible for the generation of respiratory aerosol particles have been identified in the literature, viz., coughing, sneezing, talking, and breathing. The number concentrations of emitted particles are higher in the former two mechanisms and hence are given more importance to determine transmission characteristics. Accordingly, majority of researchers have focused on coughing and sneezing in their studies.[11−15] It is also known that asymptomatic patients, who rarely cough or sneeze, transmit the disease vectors[5,16] and may be significant contributors to the overall disease load.[17] Consequently, a few recent studies have specifically studied

Received: March 19, 2021
Accepted: June 8, 2021
Published: June 23, 2021

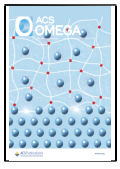

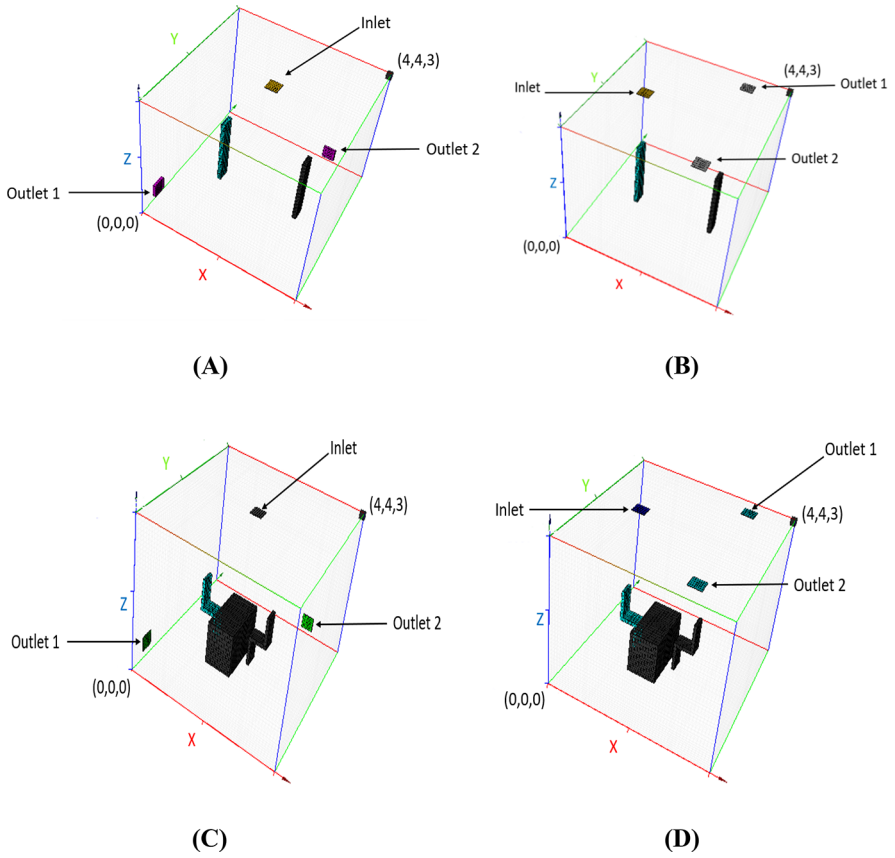

Figure 1. Arrangement of human models and inlet/outlet configurations for four scenarios, as follows: (A) standing, ceiling−wall scenario; (B) standing, ceiling−ceiling scenario; (C) sitting, ceiling−wall scenario; and (D) sitting, ceiling−ceiling scenario.

the transmission during talking as well.[18,19] The distance traveled and the residence time of aerosol plume are different for different respiratory mechanisms owing to the difference in ejection characteristics. The distance traversed by aerosol particles depends on various factors like particle size, density, existing flow pattern, and initial velocity of the exhaled/emitted particles. For a two-phase system involving transition dynamics, general interpretations for or on the basis of threshold parameters such as safe distance are dubious. Respiratory droplets of size >5 μm were shown to have a short atmospheric residence time and settle at a distance less than 1 m.[20] However, droplets in the same size range were found to be dispersed to larger distances in another study.[21] Such diverse implications are not surprising due to the interplay of characteristics of the exhaled respiratory particles and the flow dynamics. Coronavirus having a free size of 60−140 nm[22] attaches to droplets/particles in the respiratory tract and gets emitted while coughing, sneezing, talking, etc. In a study by Chia et al,[23] SARS-CoV-2-bearing particles of sizes >4 and 1−4 μm were found in air sampling inside airborne infection isolation rooms, with 12 ACH (air changes per hour).

For indoor transmission, ventilation conditions significantly influence the aerosol transport and deposition and ultimately the safe distance. Guidelines have repeatedly emphasized the role of ventilation as one of the key prevention and control measures.[14,24] The complex interplay between fluid dynamics of indoor ventilation and expiration events from infected persons might affect the strategies to mitigate the transmission of the disease.[25] Inappropriate ventilation design has been linked to inefficient particle removal, creation of local hot spots, and enhanced surface contamination for different practical settings.[26] Airflow patterns have been shown to be accountable for airborne transmission of SARS-CoV-2 in independent studies.[6,14,27] Complexities associated with airflow patterns also challenge the threshold-based approaches for defining safe distance as well as deducing general interpretations. The inefficacy of a fixed safe distance, its dependence on environmental conditions, and the recommendation to increase it beyond 2 m have been discussed in recently published studies.[14,28,29] Consistent efforts are being made to study and interpret the coupling of airflow dynamics and particle transport in varying indoor settings.[6,27,30] However, there are limited numbers of comprehensive studies that examine all major airborne transmission respiratory modes of transport vectors in an indoor environment.

Overall, parameters of the event (viral load, flow velocity), aerosol characteristics (concentration, size distribution pattern), and ventilation patterns affect the accuracies of the scientific ways employed to arrive at effective preventive policies for safe distance. Both experimental and numerical studies have helped scientific authorities and policy makers in evolving the knowledge database in the context of SARS-COV-2 and past pandemics/epidemics. Although the crucial role of ventilation has been highlighted, additional interpretations on the basis of change in airflow patterns and air exchange rate for indoor environments are worth examining to understand and issue better ventilation guidance. Among other tools for numerical analysis, computational fluid dynamics (CFD) has been employed for similar contexts.[31−36] Some of these CFD-based studies have evaluated the interpretations in terms of safe

https://doi.org/10.1021/acsomega.1c01489
ACS Omega 2021, 6, 16876−16889

Table 1. Flow Rates and Respiratory Droplet Size Distribution Parameters Used in this Study

event		mean size (μm)	GSD	number (duration of event, s)	airflow rate (m^3/s)	velocity of ejection (m/s)	number conc. (#/cm^3)	ref.
coughing	mode 1	1	1.5	3 discrete events (0.5)	0.005	11.2	5.5	53
	mode 2	80	1.5	3 discrete events (0.5)	0.005	11.2	5.5	28
sneezing		70	1.5	3 discrete events (0.5)	0.005	10.0	5.5	12,14
loud talking	mode 1	1	1.6	continuous (150)	0.0075	3.9	1.1	37
	mode 2	5	1.6	continuous (150)	0.0075	3.9	1.1	51
normal talking	mode 1	1	1.6	continuous (150)	0.0002	3.9	1.1	49
	mode 2	5	1.6	continuous (150)	0.0002	3.9	1.1	50

distance, as well.[36,11,14,28] For a simulated coughing event, it was concluded that the safe distance of 6 ft may not be sufficient due to the intricacy of the environmental conditions.[11] Although being of lesser momentum and concentration, particles ejected due to talking could amplify the infection risk due to their continuous emission and higher airborne prevalence.[37]

This study focuses on the airborne transmission/propagation of particles emitted for different respiratory events, viz., coughing, sneezing, normal talking, and loud talking, in an indoor space representing a typical closed ventilated office room. Postpandemic, as the world slowly returns to normalcy, it is important to ensure that office spaces are maintained at safe conditions to mitigate the spread of infections. Two types of ventilation patterns (inlet/outlet at ceiling/wall and ceiling/ceiling, respectively) and three different air exchange rates (4, 6, and 8 ACH) have been used for performing the simulations. Two human models are placed inside the room, 2 m apart, in two different positions, namely, standing and sitting. We used the best suitable literature-based parameters representing these events and focused on the interpretations around the concept of safe distance of 2 m. The results have been presented and discussed in a manner to bring out the intricacies involved in the role of airflow patterns on the particle transmission.

2. RESULTS AND DISCUSSIONS

This study considered two types of airflow patterns, three ventilation rates, two emitter−receiver scenarios (Figure 1), and four respiratory mechanisms (coughing, sneezing, normal talking, and loud talking). The input aerosol parameters corresponding to these mechanisms were taken from the available literature (Table 1).

Eight locations (A−H) (Figure 2) were chosen as probes at different distances from the emitter of the respiratory particles during the events as discussed above. Locations A and B were taken at 1 m distance, left and right to the emitter, respectively. Locations D and G were in the front direction from the emitter at a distance of 1 and 2 m, respectively. Locations C, F and E, H were in the left and right direction at a distance of 1 m from D and G, respectively. Location G, representing the human model receptor, was at the distance of 2 m from the emitter, and majority of results discussed henceforth are focused on this point.

Four different scenarios as shown below have been used for comparison and interpretation purposes:

1. Scenario 1 (Sc1): standing−standing position, ceiling−wall ventilation pattern
2. Scenario 2 (Sc2): standing−standing position, ceiling−ceiling ventilation pattern
3. Scenario 3 (Sc3): sitting−sitting position, ceiling−wall ventilation pattern

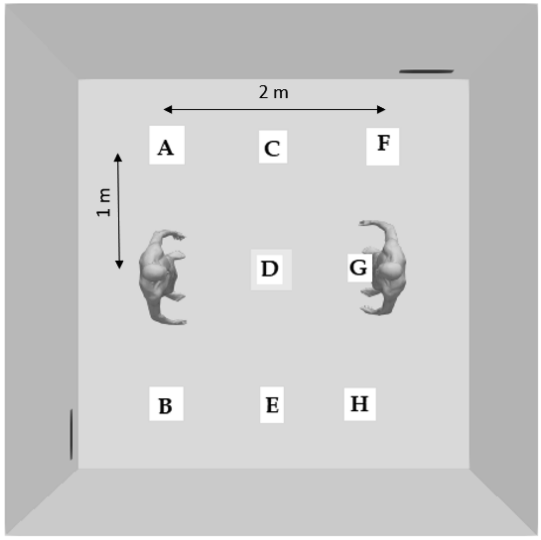

Figure 2. Probe locations used for postprocessing of simulation results.

4. Scenario 4 (Sc4): sitting−sitting position, ceiling−ceiling ventilation pattern

For Sc1 and Sc2, probes are located at a height of 1.5 m, same as the height of ejection of particles at the emitter. In the other positioning configurations (Sc3 and Sc4), probes are located at 1.14 m, corresponding to the height of the emitter in the sitting position. Results for the simulations conducted under this work have been presented in three parts. In the first part, variations in the evolution of the particle number concentration profile for all respiratory events have been presented at a fixed air exchange rate of 4 ACH. Unless specified, we focus on the location of the receptor (location G) and for the simulation time of 10 min. The evolution profiles have been interpreted with the help of airflow patterns in the simulation domain. Subsequently, in the second part, we discuss the effects of variation of air exchange rate for a loud talking event. Finally, we present results of some follow-up simulations (extremely low air exchange rate of 0.5 ACH, simulation for 30 min) for additional inferences.

For each of the ventilation and emitter−reception configuration scenarios (Sc1−4), an initial steady-state flow is computed for each air exhange rate (4, 6, and 8 ACH).Figure 4A−D shows contours of this initial steady flow on a vertical center plane for all four scenarios, Sc1−4, for the air exchange rate of 4 ACH. This steady-state flow is then the initial condition for the transient coupled flow and particle transport simulations. The flow changes due to the volume of air ejected during each of the respiratory events, and this is captured by solving for flow in transient mode. There is a one-way coupling between the flow and particle transport, with the flow affecting the particle

https://doi.org/10.1021/acsomega.1c01489
ACS Omega 2021, 6, 16876−16889

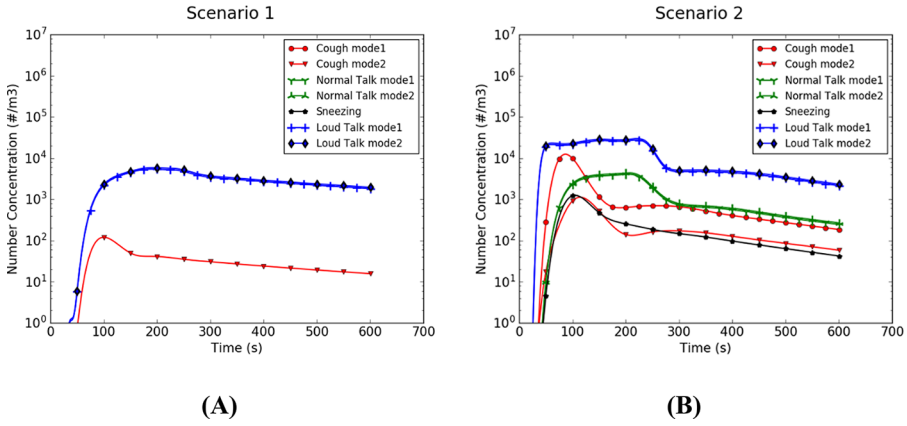

Figure 3. (A, B) Temporal evolution of the integral number concentration of aerosol particles at location G for scenarios 1 and 2 (all respiratory events).

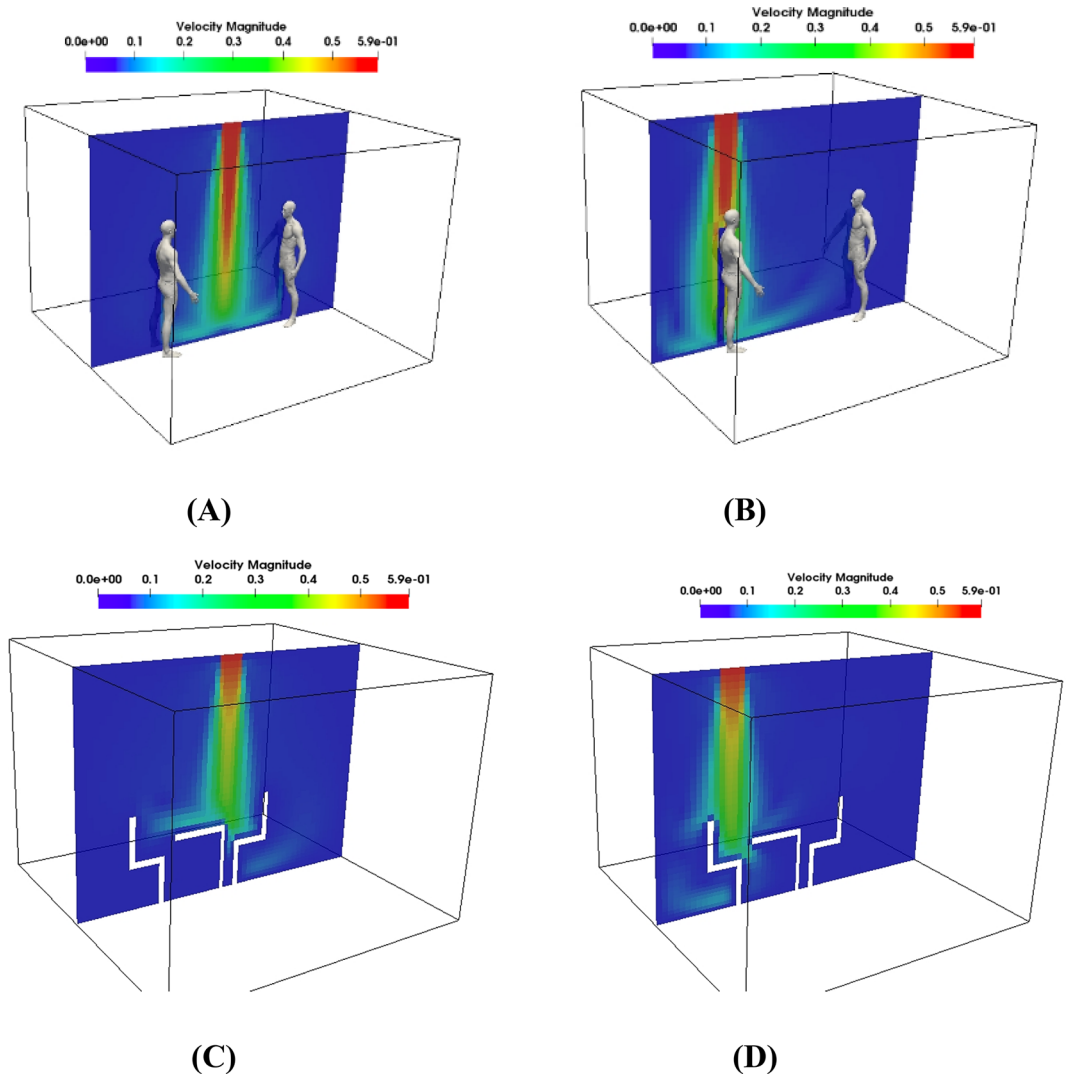

Figure 4. (A–D) Steady-state air velocity diagram for scenarios 1, 2, 3, and 4, respectively.

transport, while the particle concentration is too dilute to affect the flow.

2.1. Comparison of Different Respiratory Events at Four ACH Ventilation Rates. Figure 3A,B shows the evolution of the integral number concentration with time (10 min) at location G for Sc1 and Sc2, respectively.

As can be seen for Sc1 (Figure 3A), particles reached the receptor at G only for three out of seven respiratory events. The number concentration for loud talking (for both size modes) was seen to be increasing to 5.39E3/m^3 and then decreasing slowly afterward. Particles corresponding to coughing mode 2 were also seen to be reaching the receptor. But the peak number

https://doi.org/10.1021/acsomega.1c01489
ACS Omega 2021, 6, 16876−16889

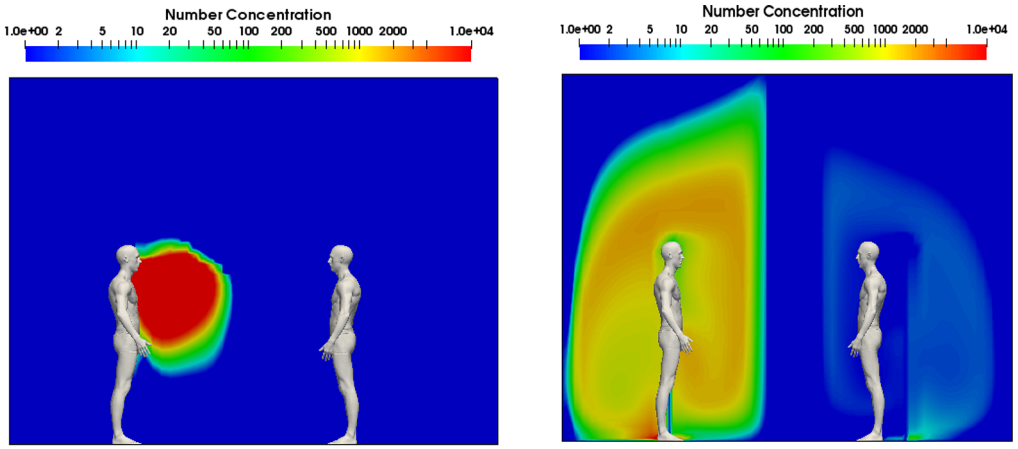

Figure 5. (A, B) Snapshots of the number concentration contour (at vertical midplane) for sneezing in Sc1 at 2 and 190 s.

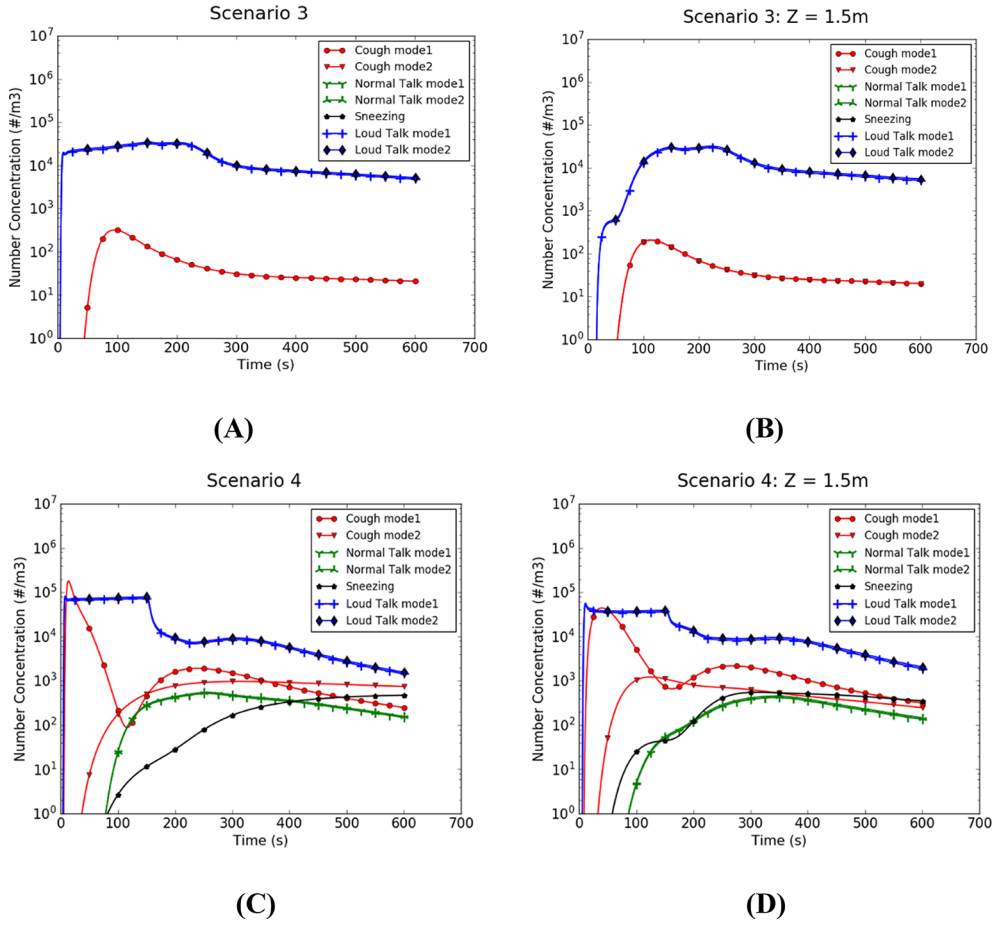

Figure 6. (A–D) Temporal evolution of the integral number concentration of aerosol particles at location G for for scenarios 3 and 4 (all respiratory events).

concentration for this case was found to be 1.19E2/m^3, much less than that of loud talking. On the contrary, the number concentration evolution profile was seen to be evolving for all seven events for Sc2 (Figure 3B). The behavior of the concentration profile was found to be similar for normal talking and loud talking. Whereas the number concentrations for both the modes for these two events were observed to follow each other closely, a clear difference could be noted for coughing modes 1 and 2. This was expected as both the modes for normal as well as loud talking (1 and 5 μm) are close enough so as to not set any settling-induced difference in the evolution profile. The maximum number concentration (2.84E4/m^3) for this scenario was obtained for loud talking, similar to Sc1. The next event showing a high number concentration was coughing mode 1

https://doi.org/10.1021/acsomega.1c01489
ACS Omega 2021, 6, 16876−16889

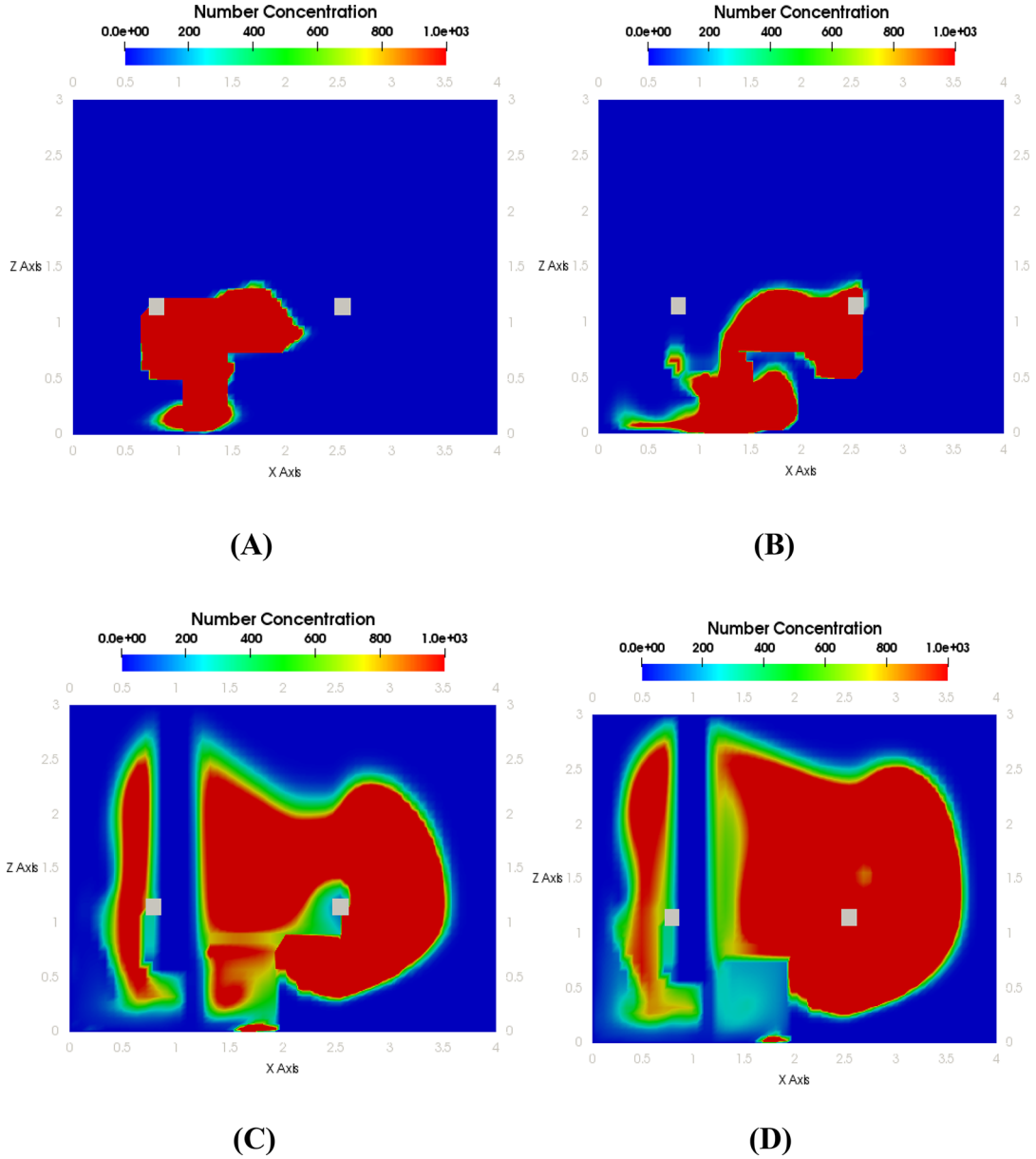

Figure 7. (A−D) Snapshots of the number concentration contour (at vertical midplane) at 3, 10, 96, and 200 s obtained for coughing mode 1 for Sc4.

(1.24E4/m^3), although the number concentration was seen to be higher for normal talking (both modes) at late times. These differences (as observed for Sc1 and Sc2) can be further interpreted on the basis of steady-state air velocity vector profile. These profiles plotted for vertical midplane passing between the human subjects (at $Y = 2$) have been depicted in Figure 4A,B.

The absence of particles for some events for Sc1 at location G can be understood on the basis of Figure 4A. There is an existing barrier or curtain of flow stream due to the ventilation pattern emanating from the inlet and forming the air circulation pattern for the conditions prevalent due to the outlet position and the ventilation rate. This curtain does not allow the particles with low flow velocities and small momentum to cross it. The strength also depends on the closeness to the emitter because the particles emitted with their maximum velocity lose their strength (velocity magnitude) as they travel farther. So, Sc1 in addition to the strong flow barrier is far from the source (emitter), hence leading to the maximum relative strength. Because of this barrier, particles are expected to take time to reach the receptor, which was signified by the late pickup of the number concentration for Sc1. Due to these reasons dependent on flow conditions in Sc1, only particles due to loud talking (maximum exit flow velocity) and due to coughing reached location G. For the coughing event, only the higher mode (80 μm) penetrated this barrier. Although the particle size generated due to the sneezing event was close to coughing mode 2, ejection at 30° below the horizontal axis resulted in its faster deposition. This can be validated from Figure 5, which shows the particle plume generated due to sneezing at 2 and 190 s, respectively. In comparison to Figure 4A, Figure 4B clearly demarcates the role of the air curtain in allowing/inhibiting particles to reach the receptor. As the air curtain for Sc2 was near the emitter, even low exit flow rates/exit velocities were sufficient for particles to penetrate the barrier and hence reach the receptor.

For the sitting−sitting configuration (Sc3 and Sc4), the temporal evolution of the integral number concentration of particles at location G at a height of 1.14 m, corresponding to different events, has been represented in Figure 6A−C. The

https://doi.org/10.1021/acsomega.1c01489
ACS Omega 2021, 6, 16876−16889

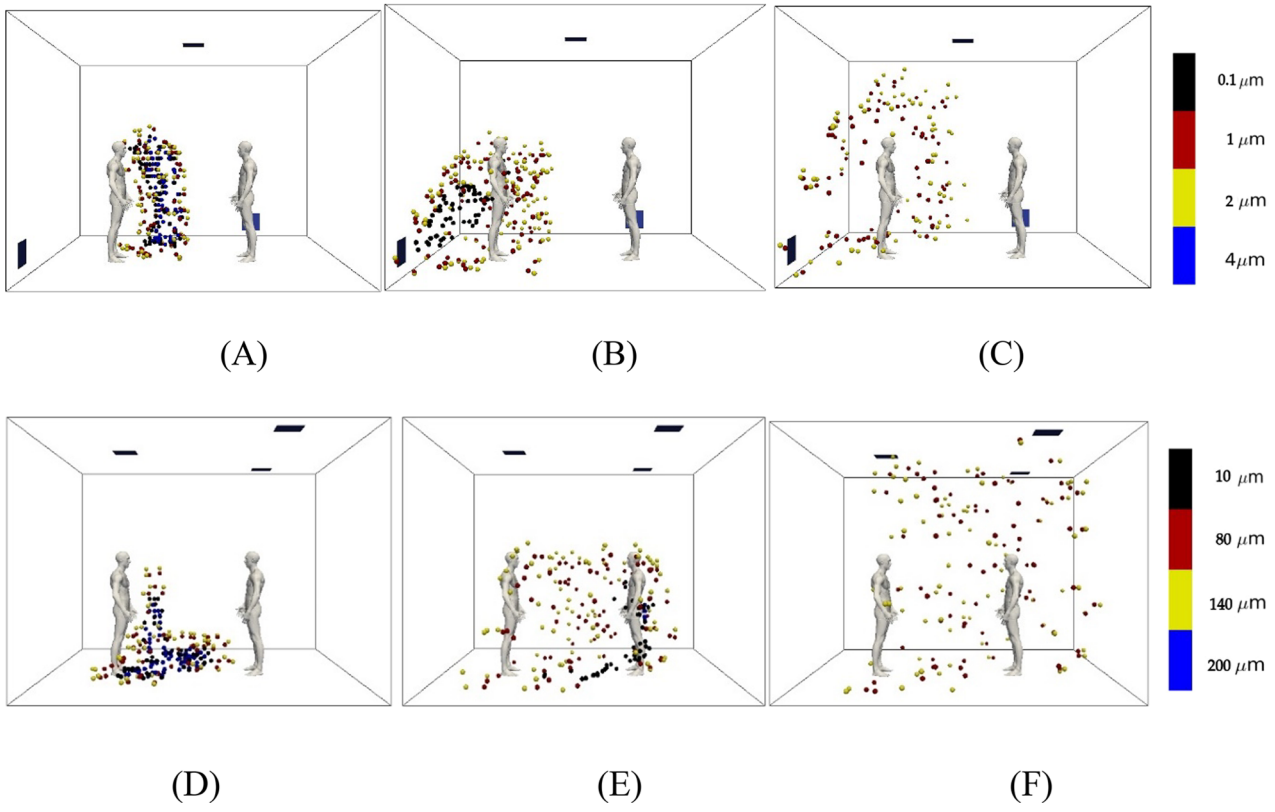

Figure 8. Particle size distribution evolution of (A−C) coughing mode 1 for Sc1 at 10, 50, and 220 s, respectively, and (D−F) coughing mode 2 for Sc2 at 10, 50, and 200 s, respectively.

steady-state air velocity vector profile corresponding to Sc3 and Sc4 has been plotted as Figure 4C,D.

Barring some differences, the number concentration evolution pattern corresponding to Sc3 and Sc4 is more or less similar to that shown for Sc1 and Sc2, respectively. Sc3 also has an air curtain barrier similar to Sc1 but of less magnitude (Figure 4A,C). It also has an additional obstruction in the form of the table. Particles generated due to loud talking almost instantaneously reached the receptor for this case. However, particles generated due to coughing with a relatively lower flow rate took some time to reach the receptor. Another difference between Sc1 and Sc3 is the presence of cough mode 2 in the former and cough mode 1 in the latter. The absence of cough mode 2 in Sc3 can be attributed to the deposition of these particles, as the emission for this case occurred at the height of 1.14 m very close to the table surface. We also analyzed the behavior of particles at the height of 1.5 m for Sc3 and Sc4 (Figure 6B,D). For this case, the air curtain profile changed, but the presence of the source at 1.14 m had no significant effect on the overall trends. Therefore, any difference seen for the case of Sc3 and Sc4 in comparison to other two cases could not be attributed to the difference of the height of probes.

It is needless to mention here that CFD analysis makes it possible to visualize short-term and long-term features that could be of interest but restrictive to measure experimentally. For example, the observed temporal evolution for the number concentration of particles generated due to coughing (mode 1) for Sc4 was entirely different from that of the other three scenarios. It showed an instantaneous increase in concentration at early times leading to the first mode, followed by the second mode after 200 s of ejection. Figure 7A−D demonstrates the same in the snapshots taken from the number concentration evolution profile at different times for this case. It can be noted that particles were emitted till 3 s and reached the receptor at around 10 s (Figure 7B). This corresponded to the observance of the first hump as shown in Figure 6C. This was followed with a lesser concentration zone formed around the receptor at 96 s (Figure 7C). However, the number concentration around the receptor again increased close to 200 s (Figure 7D), resulting in a bimodal curve (Complete Movie S1; available in the Supporting Information). This is different with respect to the case of loud talking, wherein the number concentration quickly reached steady state and thereafter decreased after the source was off. As loud talking is the event corresponding to the highest flow rate, it is least affected by the ventilation patterns specifically with regard to sporadic fluctuations. The airflow patterns corresponding to the event in such cases dominate over the room ventilation pattern during the progression of the event as demonstrated by the simulations.

The results from the simulations also support the conclusions of the studies and recent policy guidelines[38,39] that "threshold based safe distance quantifications" cannot be a general prevention approach. As clearly seen, the exposure of the receptor not only depends on the characteristics of the respiratory events, but it strongly gets influenced by the external conditions around the emitter and the receptor. Whereas only three out of seven events resulted in the exposure of the receptor for Sc1 and Sc3, all seven events breached the 2 m limit for Sc2 and Sc4. Although the inferences evolved on the basis of the above discussion depend on the inlet−outlet positions and the air exchange rate (specific to the design of this study), some general conclusions can be drawn. As stated above, any effort in the direction of marking safe distance and linking mitigation strategies to the same should be exhaustive in terms of inclusion

https://doi.org/10.1021/acsomega.1c01489
ACS Omega 2021, 6, 16876−16889

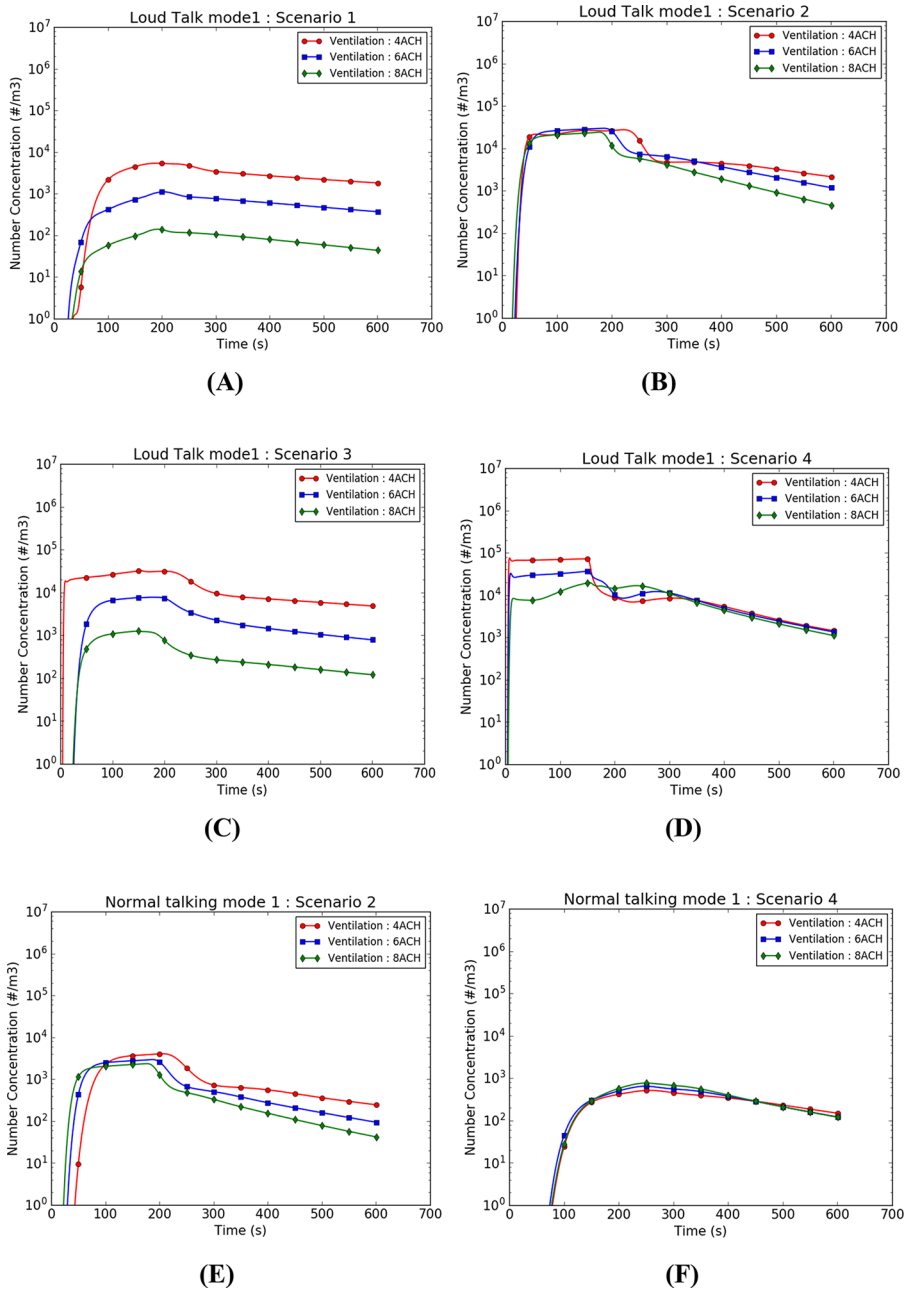

Figure 9. Temporal evolution of number concentration (at location G) as a function of ventilation rate for (A−D) loud talking mode 1 for all scenarios and (E, F) normal talking mode 1 Sc2 and Sc4.

of sensitive variables. Inlet−outlet configurations studied in this work indicate that "air curtains" as a design engineering feature could be an appropriate choice for indoor settings. Air circulation from top/bottom to sidewalls can form such air curtains for closed ventilated spaces. The observance of particles at the location of the receptor for normal talking for some cases is imperative as well. Given the role of asymptomatic patients in the transmission of infection, more studies in this direction could be an important contribution.

The size distribution evolution of particles generated from the emitter has been depicted in Figure 8A−C and D−F for coughing mode 1 (Sc1) and coughing mode 2 (Sc2), respectively (Complete Movies S2 and S3; available in the Supporting Information). For simplicity, only four particle sizes are chosen for visual interpretation, which are 0.1, 1, 2, and 4 μm for coughing mode 1 (Sc1) and 10, 80, 140, and 200 μm for coughing mode 2 (Sc2). The dots shown in these figures appear only when the number particle concentration is more than $1/m^3$. As evident, particles generated for coughing mode 1 in Sc1 redistribute around the emitter, leading to the removal of large particles by gravitation settling and of other particles by ventilation (Figure 8A−C). However, these particles do not reach the receptor for the existing room conditions and the ventilation pattern. This is different from the time history shown in Figure 8D−F for large-sized coughing mode 2 in Sc2. Although the settling-induced deposition affected the concentrations for the higher sizes, particles of all sizes engulfed the surroundings of the receptor due to a weaker barrier of flow compared to Sc1.

https://doi.org/10.1021/acsomega.1c01489
ACS Omega 2021, 6, 16876−16889

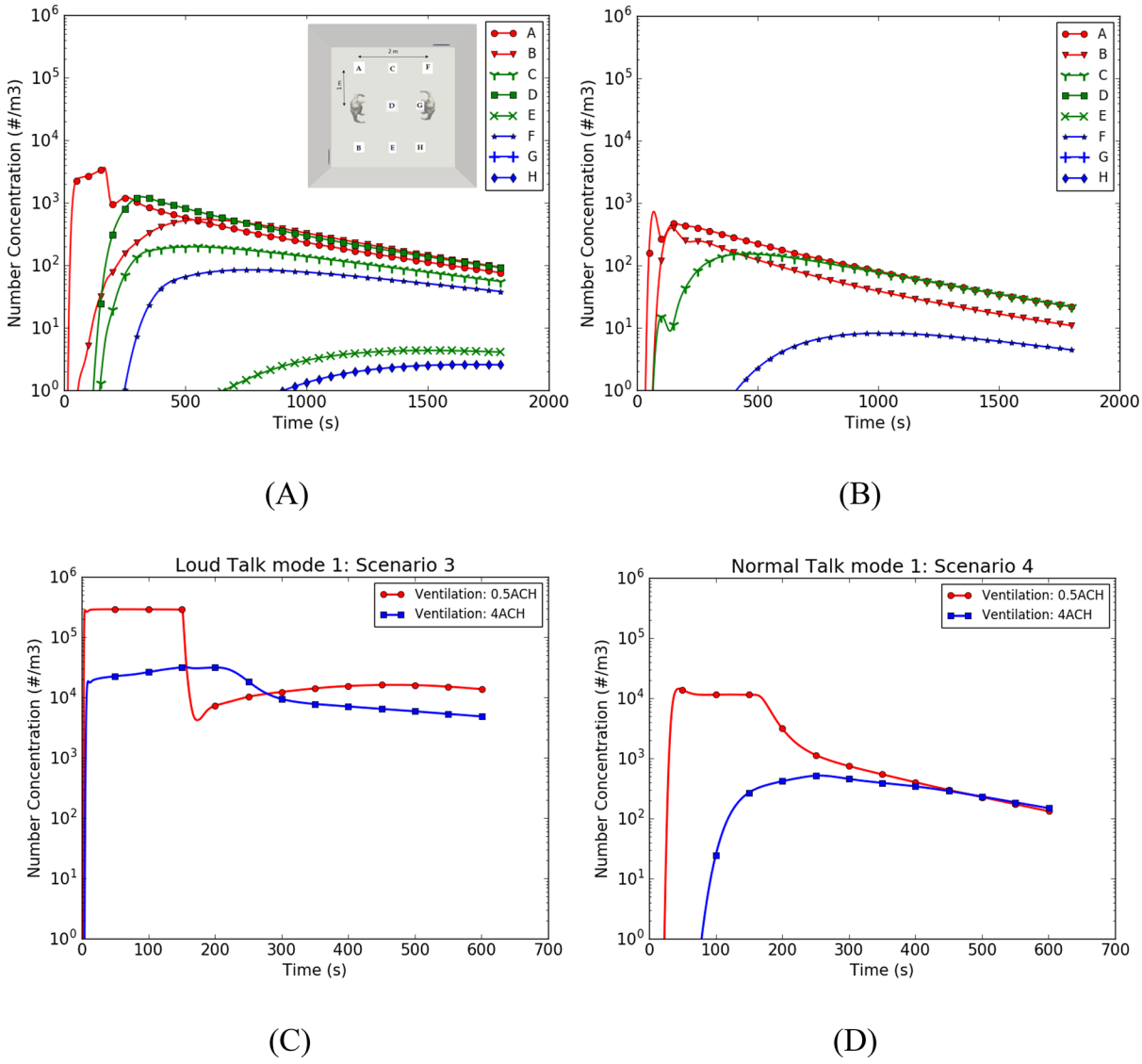

Figure 10. Temporal evolution of the number concentration of particles for additional supplementary simulations at (A) locations A−G for simulation time of 30 min at 4 ACH for normal talking mode 1, Sc3; (B) locations A−G for simulation time of 30 min at 4 ACH for coughing mode 1, Sc1; (C) location G, 0.5 and 4 ACH ventilation rate for loud talking mode 1, Sc3; and (D) location G, 0.5 and 4 ACH ventilation rate for normal talking mode 1, Sc4.

2.2. Effect of Ventilation Rate on the Evolution of Number Concentration. Three air exchange rates (4, 6, and 8 ACH) were chosen to study and interpret the effect on the number concentration evolution profile for loud talking mode 1 (event present in all scenarios and with maximum concentration). The comparative patterns for all four scenarios have been shown in Figure 9A−D, respectively.

As evident and as expected, the number concentration decreased with an increase of the ventilation rate due to ventilation removal in Sc1 and Sc3. But contrary to the general tendency, this ventilation-based trend was not followed in Sc2 and Sc4. For Sc2, the number concentration profile was found to be independent of the ventilation rate till the event was in progress (0−150 s). Afterward, the behavior became similar to Sc1 and Sc3, resulting in a lesser number concentration for a higher ventilation rate. Interestingly, the pattern got reversed in Sc4 (in comparison to Sc2), showing the differences for the first 150 s and then becoming independent of the ventilation rates. For the case of Sc2, this behavior can be explained on the basis of the interplay between the flow velocity patterns of the emitter and the room. As shown earlier, the air curtain barrier was weaker for Sc2, and the coupling of the same with higher flow rates corresponding to loud talking and closeness of the barrier to the emitter negates any role of room ventilation patterns till the time the event is progressing. This means that the ventilation rate had no role to play till 150 s and then it affected the profiles as expected. For the case of Sc4, the relatively strong air curtain barrier ensured that the ventilation rate dominates the evolution patterns in comparison to the event-induced airflow pattern till 150 s. But once the event stops, the concentration profile becomes independent of the ventilation rate due to the fact that the effect of ventilation is not reaching the receiver as can be seen from the flow profile of Sc4 (Figure 8B) due to the obstruction by the table. This reasoning was validated when we plotted similar curves for all scenarios replacing loud talking by normal talking. As can be seen in Figure 9E,F, when the airflow fields generated by the events were weakened, the profiles get influenced by room ventilation patterns. The number

https://doi.org/10.1021/acsomega.1c01489
ACS Omega 2021, 6, 16876−16889

concentration profile was seen to be dependent on the ventilation rate in Sc2 and independent in Sc4 as expected because of hindrance by the table. The study reiterates the role of ventilation toward the evolution of the number concentration of particles in a closed environment. For the chosen scenarios, sitting−sitting configurations (Sc3 and Sc4) also showed nonconformance to the generalized ventilation-based removal behavior (increase in removal for higher ventilation rates). This kind of behavior has also been highlighted in few other studies[40] and challenges the generalized notion to use ″increase in ventilation removal″ as a mitigation measure.[24]

2.3. Some Additional Inferences. In addition to the simulations as per the designed test matrix, we studied two additional aspects, viz., relatively longer-term evolution and the patterns at an extremely small flow rate representative of a closed indoor environment without any external forced flow. We selected normal talking mode 1, Sc3 and coughing mode 1, Sc1 for investigating number concentration profiles generated due to the simulations performed for 30 min. Evolution patterns as a result of these simulations have been interpreted at all locations (A−G) of the computational domain for this case. It was intuitive to probe coughing mode 1 for Sc1 in this additional run as it was seen to be not reaching the receptor till the simulation time of 10 min (compared to mode 2 of the same event). The results for these long-term simulations are shown in Figure 10A,B for coughing mode 1 (Sc1) and normal talking mode 1 (Sc3), respectively. As seen from Figure 10A, particles emitted from the emitter could not reach the receptor within 30 min. However, a buildup of concentration can be seen at other locations, specifically A−E. A buildup can also be observed at E, F, and H locations at later times. In comparison, the number concentration was observed to be more than $1/m^3$ for coughing case at only four locations up to 30 min.

For observing the effect of extremely low ventilation rate (0.5 ACH), the number concentration evolution has been compared for 0.5 and 4 ACH for loud talking mode 1, Sc3 and normal talking mode 1, Sc4, respectively (Figure 10C,D). As expected, the poor ventilation resulted in higher number concentrations for both the selected cases. Again, in case of Sc4 (Figure 10D), after 300 s, the concentration profile becomes independent of the ventilation rate similar to that seen in Figure 9D. Concentration profiles for the two ACHs are dissimilar during the initial time due to the relative strength of the emitted particles. Though the flow rate of the emitted particles is less with respect to 0.5 ACH, it becomes substantial and hence dominates the existing ventilation. The results from the additional simulations also revalidate the findings made on the basis of main test cases mainly in terms of complexities in interplay between the event ejection flow dynamics and the existing and evolving airflow patterns of the indoor environment.

3. METHODS

In this study, respiratory droplets are modeled as size distributed particle phase that is transported and diffused in the airflow within the indoor setting, i.e., closed and mechanically ventilated office space. We used the ANSWER CFD code[41] to solve the coupled problem of flow and respiratory particle transport. This code solves the full 3D Navier−Stokes equation for arbitrary grids using the Finite Volume Method. It has a variety of Reynolds-Averaged Navier−Stokes (RANS)-based models, Reynolds Stress models, and Large Eddy Simulation models (LES) for modeling fluid turbulence. For all simulations in this study, the RANS-type standard *k*-epsilon turbulence model is used for closure. The CFD framework of this code has been coupled to the modules written for aerosol transport and dynamics by our research group as shown below.[42−44]

$$\frac{\partial n(d_p, r, t)}{\partial t} + \nabla.\,[Un(d_p, r, t)] = \nabla.\,\{D(r, t)\nabla n(d_p, r, t)\}\frac{+1}{2}\int_0^{d_p} K(d'_p, d_p - d'_p)n(d'_p, r, t)n(d_p - d'_p, r, t)d(d'_p) - n(d_p, r, t)\int_0^{\infty} K(d_p, d'_p)n(d'_p, r, t)d(d'_p) + S(d_p, r, t) - \lambda n(d_p, r, t) - \nabla.\,[U_{drift}n(d_p, r, t)] \quad (1)$$

where d_p and d'_p are particle diameters; $n(d_p, r, t)$ is the spatially (r) and temporally (t) varying number concentration distribution function for particle diameter d_p; U is the gas phase velocity; D is the particle diffusivity; K is the collision frequency between particles of different sizes; S is the source term arising from nucleation and direct emission; λ is the decay rate of the species; and U_{drift} is the total drift velocity of the aerosol particles due to various mechanisms like gravitational settling, thermophoresis, etc. Equation 1 is a partial integro-differential equation, where the integrals on the right-hand side are terms for the (a) formation of new particles from collision of existing particles and (b) depletion of an existing particle by collision with another particle. The code has options to use different forms of collision frequency kernel including the Fuchs kernel. A sectional method[45] has been implemented in the aerosol module for the numerical solution of eq 1. The particle diffusivity shown in eq 1 is also a function of particle size and is given by:

$$D = \frac{k_b T C_c}{3\pi\mu_g d_p} \quad (2)$$

where k_b is the Boltzmann constant, T is the temperature, μ_g is the gas viscosity, and C_c is the Cunningham slip factor[46] given by:

$$C_c = 1 + Kn^*\,(2.514 + 0.8^*\exp(-0.55/Kn)) \quad (3)$$

In the above equation, Kn (Knudsen number) is the ratio of the mean free path of the gas particles (λ) to the particle radius ($d_p/2$) and is given as:

$$Kn = \frac{2\lambda}{d_p} \quad (4)$$

The aerosol particles undergo settling and deposition due to gravitational forces. Gravitational settling modeled as a drift flux velocity in the code can be written as:[47,48]

$$v_g = g\tau \quad (5)$$

with τ as the relaxation time,

$$\tau = \frac{C_c\rho_g d_p^2}{18\mu_g} \quad (6)$$

ρ_g in the above equation denotes gas density. For the size of particles under consideration, the Stokes number is <1 and inertial effects can be ignored. As the number concentration is

https://doi.org/10.1021/acsomega.1c01489
ACS Omega 2021, 6, 16876−16889

low, coagulation has also been neglected. Therefore, gravitational settling is the only drift flux considered in this study. More details about the aerosol modules, numerical scheme, and validations (analytical, numerical, and experimental) can be found elsewhere.[42−44]

3.1. Problem Description. The problem under consideration is the exposure of an uninfected person (receptor) to the COVID-19 virus due to respiratory droplets emitted from an infected person (emitter) in an indoor office setting under a variety of mechanical ventilation conditions. Virus-carrying respiratory droplets are produced by the emitter during various events including normal exhalation and conversation, i.e., talking, loud conversation (or loud talking), coughing, and sneezing. These may be in the range of sizes from submicron to hundreds of micrometers, comprise saliva and mucus, and are ejected out along with the stream of exhaled or ejected air. Each of these events is considered in this study as part of a matrix of hypothetical scenarios.

3.2. Computational Domain, Grid, and Preprocessing. The computational domain used for performing simulations is a typical office room of dimensions 4 × 4 × 3 m. This domain is represented as a cuboidal box spanning from ($X = 0, Y = 0, Z = 0$) to ($X = 4, Y = 4, Z = 3$). This domain was discretized with 144,000 hexahedral cells with grid clustering near the walls and the human models. The cell sizes vary in size between 2 mm (next to wall) and 75 mm away from any obstructions or walls. In the cases/scenarios taken under this study, two human models are placed inside the room, 2 m apart, in two different positions, namely, standing and sitting positions. For the first position, i.e., standing scenario, humans are modeled as a cuboidal block of size 0.1 × 0.3 m cross section and 1.6 m height. These human models are placed facing each other and centered at floor coordinates ($X = 1, Y = 2$) and ($X = 3, Y = 2$). The source of exhaled/ejected air is placed at the location ($X = 1.02, Y = 2, Z = 1.5$), suggesting that respiratory droplets are released from a height of 1.5 m for this position (Figure 1A).

In the second position (sitting scenario), two human models are positioned as sitting 2 m apart, separated by a table. The humans are modeled as three separate cuboidal sections: the lower vertical portion of the leg being 0.1 × 0.3 × 0.5 m in height, the bent horizontal portion of the leg being 0.5 × 0.3 × 0.1 m in thickness, and the vertical torso portion being 0.3 × 0.1 × 0.6 m. The torso portions are placed at $X = 0.7$ and 2.7 m, respectively, giving a separation distance of 2 m. The table is of dimensions 0.7 × 1.2 × 0.8 m, consisting of three vertical portions, a top horizontal portion, and a solid drawer portion. For the sitting position, the source of exhaled/ejected air is placed at ($X = 0.72, Y = 2, Z = 1.14$), suggesting that the respiratory droplets are released from a height of 1.14 m (Figure 1C).

The airflow pattern in the room is governed by the positions of inlets and outlets, and for the present study, two configurations are chosen: ceiling−wall and ceiling−ceiling configurations. In the ceiling−wall configurations, the inlet of dimension 0.3 × 0.3 m is placed at the center of the ceiling, while two outlets, of dimension 0.45 × 0.15 m, are located on the side walls. Outlet 1 is on the $X = 0$ wall and spans from ($Y = 0.15, Y = 0.3$) to ($Y = 0.6, Y = 0.45$). Outlet 2 is located on the $Y = 4$ m wall and spans from ($X = 3.3, Z = 0.3$) to ($X = 3.75, Z = 0.45$). In the ceiling−ceiling ventilation position, there is one inlet of dimension 0.3 × 0.3 m centered at ($X = 1, Y = 2, Z = 3$). The two outlets of dimension 0.3 × 0.3 m are placed on the ceiling. One outlet is centered at ($X = 3, Y = 0.5, Z = 3$), while the other outlet is centered at ($X = 3, Y = 3.5, Z = 3$). Three different ventilation rates are considered in this study, namely, 4, 6, and 8 ACH (corresponding to volumetric airflow rate of 192, 288, and 384 m^3/h). Ventilation rates 4 and 6 ACH have been used in the literature as well.[50] For both human positions, ceiling−wall and ceiling−ceiling ventilation patterns with above-stated ventilation rates have been used in different combinations for the simulations.

3.3. Boundary Conditions and Input Parameters. The outlets are set as open boundaries with a fixed pressure of $P = 0$ for flow and zero gradient for the particles. The background concentration of respiratory droplets and that of the particles at the inlet are assumed to be zero. In addition, any background aerosol source term has been neglected for simplicity. Deposition driven by size-segregated gravitational settling velocity has been taken for the floor surface only. No deposition is assumed to take place at the vertical side walls or at the ceiling walls, and the particles are assumed to move with the flow along the wall.

As mentioned above, normal talking, loud talking, coughing, and sneezing have been considered for these simulations. Corresponding to these respiratory mechanisms, best suited values for particle size distribution (number concentration, mean size, and geometric standard deviation), exhalation flow rate, and velocity have been taken from the literature and used for all simulations (Table 1). Normal talking is a case of continuous low flow rate and low-speed ejection of air and respiratory droplets with two distinct modes of mean sizes 1 and 5 μm.[49,50] On the other hand, loud talking is different from normal talking in terms of the higher volume of ejected air, continuous ejection of air at higher flow rate but low speed, and moderate number of respiratory droplets with two distinct modes of mean sizes 1 and 5 μm.[37,51] Loud talking can also be equated with singing or speeches, signifying an increased aerosol emission with voice loudness.[52] Coughing involves high flow rate and high-speed ejection of air containing a relatively higher number of particles. However, unlike the talking events, coughing is a discrete short-duration event. Two distinct modes are reported in the literature from experiments with mean sizes of 1 and 80 μm, respectively.[53,28] Sneezing is, again, a discrete, short-duration event similar to coughing. While two modes of particle size distribution are reported in the literature for sneezing, with mean sizes of 70 and 360 μm,[12,14] the upper size mode is neglected, being too large for airborne propagation. Table 1 also shows the difference of these events in terms of the number concentration of emitted particles. As can be seen, coughing and sneezing have been characterized with a higher number concentration than talking. For each of these events, nine separate size classes based on mean and dispersion values have been considered for simulations. Normal and loud talking events have 0.1, 0.3, 0.8, 0.9, 1, 1.1, 1.3, 2, and 3 μm for mode 1 and 1, 3, 4, 5, 6, 7, 12, 18, and 25 μm for mode 2. For coughing events, mode 1 consists of size classes of 0.1, 0.3, 0.8, 0.9, 1, 1.1, 1.3, 2, and 3 μm, and mode 2 consists of size classes of 10, 20, 45, 70, 80, 90, 100, 140, and 200 μm. Sneezing has the same size classes as coughing mode 2. Temperature and relative humidity have been shown to be determining variables for such studies, as they mostly affect the rate of volatilization of respiratory droplets.[54] A significant reduction in the ejected droplet size due to evaporation has been reported and quantified.[55,56] The time scale for evaporation is short, being ∼10 ms for particles with <2 μm diameter and 12.5 s for particles of 50 μm diameter.[6] In this study, the ejected sizes are already evaporated sizes, as mostly these are based on measurements that are not in situ in nature.

https://doi.org/10.1021/acsomega.1c01489
ACS Omega 2021, 6, 16876−16889

The time scale of evaporation is also much shorter compared to the simulation times of the present study, justifying the above simplification.

3.4. Miscellaneous Simulation Details. The turbulent flow simulations were carried out using the k-ε turbulence model; an inlet turbulence intensity level of 1% and turbulent length scale of 7% of the inlet dimension (of 0.3 m) are assumed for simulations. The transient simulations were carried out with a uniform constant time step of 0.01 s for both flow and particle transport. The discretized equations are solved until the residuals are less than 10^{-6} for all variables.

3.5. Methodology and Test Matrix. For each ventilation location (inlet/outlet position), human model position (standing and sitting), and air exchange rate (4, 6, and 8 ACH), an initial steady flow was obtained. The steady-state flow was the starting condition for all subsequent simulations. Then, the coupled turbulent flow and particle transport simulations were carried out for each event. For the normal talking and loud talking scenarios, the emitter was assumed to be releasing respiratory droplets from $t = 0$ to 150 s, which represents talking continuously for 150 s. No air or particle was assumed to be ejected after this period. For the coughing and sneezing events, three discrete events of duration 0.5 s with a gap of 1 s are considered, lasting from $t = 0$ to 0.5 s, $t = 1.5$ to 2 s, and $t = 3$ to 3.5 s. The flow and particle number concentrations are then simulated for a period of 600 s in total. A time step dependence study showed very little difference in concentrations at different locations for a time step of 0.001 and 0.01 s. Based on this, the time step for all simulation was fixed at 0.01 s. The receiving human, positioned 2 m away, was not assumed to exhale any air during the entire simulations.

On the basis of preliminary results, the two high-occurrence scenarios from the test matrix, viz., normal talking mode 1 and coughing mode 1, were simulated for an extended period of 30 min or 1800 s. One high-exposure event, viz., loud talking mode 1, and one high-occurrence event of normal talking were also simulated under low ventilation flow condition of 0.5 ACH, which is representative of minimal ventilation and stagnant air.

4. CONCLUSIONS

CFD simulations were performed to study the transmission of aerosols ejected from respiratory mechanisms (coughing, sneezing, normal talking, and loud talking) in an indoor environment representative of a typical small office room space. Four typical scenarios were chosen corresponding to the variations in inlet−outlet location and emitter−receptor positions. Input parameters representing the ejection of particles due to the respiratory mechanism were taken from the literature. The negligible particle number concentration at the receptor location for some scenarios and the overall features seen in the time evolution of number concentration profiles could be explained on the basis of room airflow patterns and their interplay with the airflow changes induced due to the events for shorter time scales. Interestingly, particles were seen to be reaching the receptor (at 2 m distance) for even normal talking (lowest release velocity and particle number concentration of the respiratory events considered) for some cases. The exposure of the receptor to relatively higher number concentrations (or equivalently higher viral loads) for normal talking hints at the role of asymptomatic patients in infection transmission. The particles persist at the receptor location even at 30 min after the event, showing the danger of staying in closed environments with asymptomatic persons for long durations.

The results support the renewed view of the scientific community about the transmission of SARS-CoV-2 in aerosol form. Similar to some studies conducted in different indoor settings, the results highlight the inefficacy of the generalized "threshold based safe distance approach" as a prevention or control measure. Interpretations obtained on the basis of air velocity vectors in computational domain suggest "air curtaining" as a possible mitigation strategy. The results indicate that the ventilation designs with ceiling−sidewall configurations could be a better choice compared to ceiling−ceiling configuration for both standing and sitting positions. Outlets below the breathing height could be an optimized engineering safety feature for ventilation fittings. The results of the simulations performed with varying ventilation rates challenge the recommended guidelines of increasing the ventilation rate for better removal for some settings. Interlinking airflow profiling and particle transport for different indoor settings could be the most determining factor for the design of future indoor settings. The results are relevant in the present times when the experience of COVID-19 handling is being converted to a useful tool for the future.

■ ASSOCIATED CONTENT

Supporting Information

The Supporting Information is available free of charge at https://pubs.acs.org/doi/10.1021/acsomega.1c01489.

Total number concentration evolution profile of coughing mode 1 for Sc4 (Movie S1) (MP4)

Particle size distribution evolution of coughing mode 1 for Sc1 (Movie S2) (MP4)

Particle size distribution evolution of coughing mode 2 for Sc2 (Movie S3) (MP4)

■ AUTHOR INFORMATION

Corresponding Author

Balvinder K. Sapra − *Radiological Physics and Advisory Division, Bhabha Atomic Research Centre, Mumbai 400085, India; Homi Bhabha National Institute, Mumbai 400094, India;* orcid.org/0000-0002-1666-5635; Phone: +91-25592209; Email: bsapra@barc.gov.in

Authors

Mariam − *Radiological Physics and Advisory Division, Bhabha Atomic Research Centre, Mumbai 400085, India*

Ashish Magar − *CFDVR Institute, Dharamshala, Himachal Pradesh 176219, India*

Manish Joshi − *Radiological Physics and Advisory Division, Bhabha Atomic Research Centre, Mumbai 400085, India*

Pachalla S. Rajagopal − *ACRi Infotech Pvt. Ltd., Bangalore 560037, India*

Arshad Khan − *Radiological Physics and Advisory Division, Bhabha Atomic Research Centre, Mumbai 400085, India*

Madhukar M. Rao − *ACRi Infotech Pvt. Ltd., Bangalore 560037, India*

Complete contact information is available at: https://pubs.acs.org/10.1021/acsomega.1c01489

Notes

The authors declare no competing financial interest.

https://doi.org/10.1021/acsomega.1c01489
ACS Omega 2021, 6, 16876−16889

REFERENCES

(1) *Social Distancing* https://www.cdc.gov/coronavirus/2019-ncov/prevent-getting-sick/social-distancing.html (accessed May 12, 2021).

(2) *Social distancing: what you need to do - Coronavirus (COVID-19) - NHS* https://www.nhs.uk/conditions/coronavirus-covid-19/social-distancing/what-you-need-to-do/ (accessed May 12, 2021).

(3) Advice for the public https://www.who.int/emergencies/diseases/novel-coronavirus-2019/advice-for-public (accessed May 12, 2021).

(4) Rahman, H. S.; Aziz, M. S.; Hussein, R. H.; Othman, H. H.; Salih Omer, S. H.; Khalid, E. S.; Abdulrahman, N. A.; Amin, K.; Abdullah, R. The Transmission Modes and Sources of COVID-19: A systematic review. *Int. J. Surg. Open.* **2020**, *26*, 125−136.

(5) Katelaris, A. L.; Wells, J.; Clark, P.; Norton, S.; Rockett, R.; Arnott, A.; Sintchenko, V.; Corbett, S.; Bag, S. K. Epidemiologic Evidence for Airborne Transmission of SARS-CoV-2 during Church Singing, Australia, 2020. *Emerg. Infect. Dis.* **2021**, *27*, 1677.

(6) Li, Y.; Qian, H.; Hang, J.; Chen, X.; Cheng, P.; Ling, H.; Wang, S.; Liang, P.; Li, J.; Xiao, S.; Wei, J.; Liu, L.; Cowling, B. J.; Kang, M. Probable Airborne Transmission of SARS-CoV-2 in a Poorly Ventilated Restaurant. *Build. Environ.* **2021**, *196*, 107788.

(7) Anderson, E. L.; Turnham, P.; Griffin, J. R.; Clarke, C. C. Consideration of the Aerosol Transmission for COVID-19 and Public Health. *Risk Anal.* **2020**, *40*, 902−907.

(8) Greenhalgh, T.; Jimenez, J. L.; Prather, K. A.; Tufekci, Z.; Fisman, D.; Schooley, R. Ten Scientific Reasons in Support of Airborne Transmission of SARS-CoV-2. *Lancet (London, England)* **2021**, *397*, 1603−1605.

(9) Infection prevention and control of epidemic-and pandemic prone acute respiratory infections in health care https://www.who.int/publications/i/item/infection-prevention-and-control-of-epidemic-and-pandemic-prone-acute-respiratory-infections-in-health-care (accessed May 12, 2021).

(10) Fennelly, K. P. Particle Sizes of Infectious Aerosols: Implications for Infection Control. *Lancet Respir. Med.* **2020**, *8*, 914−924.

(11) Feng, Y.; Marchal, T.; Sperry, T.; Yi, H. Influence of Wind and Relative Humidity on the Social Distancing Effectiveness to Prevent COVID-19 Airborne Transmission: A Numerical Study. *J. Aerosol Sci.* **2020**, *147*, 105585.

(12) Han, Z. Y.; Weng, W. G.; Huang, Q. Y. Characterizations of Particle Size Distribution of the Droplets Exhaled by Sneeze. *J. R. Soc., Interface* **2013**, *10*, 20130560.

(13) Lindsley, W. G.; Pearce, T. A.; Hudnall, J. B.; Davis, K. A.; Davis, S. M.; Fisher, M. A.; Khakoo, R.; Palmer, J. E.; Clark, K. E.; Celik, I.; Coffey, C. C.; Blachere, F. M.; Beezhold, D. H. Quantity and Size Distribution of Cough-Generated Aerosol Particles Produced by Influenza Patients during and after Illness. *J. Occup. Environ. Hyg.* **2012**, *9*, 443−449.

(14) Pendar, M. R.; Páscoa, J. C. Numerical Modeling of the Distribution of Virus Carrying Saliva Droplets during Sneeze and Cough. *Phys. Fluids* **2020**, *32*, 083305.

(15) Yang, S.; Lee, G. W. M.; Chen, C. M.; Wu, C. C.; Yu, K. P. The Size and Concentration of Droplets Generated by Coughing in Human Subjects. *J. Aerosol Med. Depos. Clear. Eff. Lung* **2007**, *20*, 484−494.

(16) Charlotte, N. High Rate of SARS-CoV-2 Transmission Due to Choir Practice in France at the Beginning of the COVID-19 Pandemic. *J. Voice* **2020**, DOI: 10.1016/j.jvoice.2020.11.029.

(17) Johansson, M. A.; Quandelacy, T. M.; Kada, S.; Prasad, P. V.; Steele, M.; Brooks, J. T.; Slayton, R. B.; Biggerstaff, M.; Butler, J. C. SARS-CoV-2 Transmission from People without COVID-19 Symptoms. *JAMA Netw. Open* **2021**, *4*, e2035057.

(18) Stadnytskyi, V.; Bax, C. E.; Bax, A.; Anfinrud, P. The Airborne Lifetime of Small Speech Droplets and Their Potential Importance in SARS-CoV-2 Transmission. *Proc. Natl. Acad. Sci. U. S. A.* **2020**, *117*, 11875−11877.

(19) Echternach, M.; Gantner, S.; Peters, G.; Westphalen, C.; Benthaus, T.; Jakubaß, B.; Kuranova, L.; Döllinger, M.; Kniesburges, S. Impulse Dispersion of Aerosols during Singing and Speaking: A Potential COVID-19 Transmission Pathway. *Am. J. Respir. Crit. Care Med.* **2020**, 1584−1587.

(20) Kutter, J. S.; Spronken, M. I.; Fraaij, P. L.; Fouchier, R. A.; Herfst, S. Transmission Routes of Respiratory Viruses among Humans. *Curr Opin Virol.* **2018**, 142−151.

(21) Fernstrom, A.; Goldblatt, M. Aerobiology and Its Role in the Transmission of Infectious Diseases. *J. Pathog.* **2013**, *2013*, 1−13.

(22) Zhu, N.; Zhang, D.; Wang, W.; Li, X.; Yang, B.; Song, J.; Zhao, X.; Huang, B.; Shi, W.; Lu, R.; Niu, P.; Zhan, F.; Ma, X.; Wang, D.; Xu, W.; Wu, G.; Gao, G. F.; Tan, W. China Novel Coronavirus Investigating and Research Team. A Novel Coronavirus from Patients with Pneumonia in China, 2019. *N. Engl. J. Med.* **2020**, *382*, 727.

(23) Chia, P. Y.; Coleman, K. K.; Tan, Y. K.; Ong, S. W. X.; Gum, M.; Lau, S. K.; Lim, X. F.; Lim, A. S.; Sutjipto, S.; Lee, P. H.; Son, T. T.; Young, B. E.; Milton, D. K.; Gray, G. C.; Schuster, S.; Barkham, T.; De, P. P.; Vasoo, S.; Chan, M.; Ang, B. S. P.; Tan, B. H.; Leo, Y. S.; Ng, O. T.; Wong, M. S. Y.; Marimuthu, K.; Lye, D. C.; Lim, P. L.; Lee, C. C.; Ling, L. M.; Lee, L.; Lee, T. H.; Wong, C. S.; Sadarangani, S.; Lin, R. J.; Ng, D. H. L.; Sadasiv, M.; Yeo, T. W.; Choy, C. Y.; Tan, G. S. E.; Dimatatac, F.; Santos, I. F.; Go, C. J.; Chan, Y. K.; Tay, J. Y.; Tan, J. Y. L.; Pandit, N.; Ho, B. C. H.; Mendis, S.; Chen, Y. Y. C.; Abdad, M. Y.; Moses, D. Detection of Air and Surface Contamination by SARS-CoV-2 in Hospital Rooms of Infected Patients. *Nat. Commun.* **2020**, *11*, 2800.

(24) Morawska, L.; Cao, J. Airborne Transmission of SARS-CoV-2: The World Should Face the Reality. *Environ. Int.* **2020**, *139*, 105730.

(25) Bourouiba, L. The Fluid Dynamics of Disease Transmission. *Annu. Rev. Fluid Mech.* **2021**, *53*, 473.

(26) Shao, S.; Zhou, D.; He, R.; Li, J.; Zou, S.; Mallery, K.; Kumar, S.; Yang, S.; Hong, J. Risk Assessment of Airborne Transmission of COVID-19 by Asymptomatic Individuals under Different Practical Settings. *J. Aerosol Sci.* **2021**, *151*, 105661.

(27) Lu, J.; Gu, J.; Li, K.; Xu, C.; Su, W.; Lai, Z.; Zhou, D.; Yu, C.; Xu, B.; Yang, Z. COVID-19 Outbreak Associated with Air Conditioning in Restaurant, Guangzhou, China, 2020. *Emerg. Infect. Dis.* **2020**, *26*, 1628−1631.

(28) Dbouk, T.; Drikakis, D. On Coughing and Airborne Droplet Transmission to Humans. *Phys. Fluids* **2020**, *32*, 053310.

(29) Setti, L.; Passarini, F.; De Gennaro, G.; Barbieri, P.; Perrone, M. G.; Borelli, M.; Palmisani, J.; Di Gilio, A.; Piscitelli, P.; Miani, A. Airborne Transmission Route of Covid-19: Why 2 Meters/6 Feet of Inter-Personal Distance Could Not Be Enough. *Int J Env Res Pub He.* **2020**, *17*, 2932.

(30) Vuorinen, V.; Aarnio, M.; Alava, M.; Alopaeus, V.; Atanasova, N.; Auvinen, M.; Balasubramanian, N.; Bordbar, H.; Erästö, P.; Grande, R.; Hayward, N.; Hellsten, A.; Hostikka, S.; Hokkanen, J.; Kaario, O.; Karvinen, A.; Kivistö, I.; Korhonen, M.; Kosonen, R.; Kuusela, J.; Lestinen, S.; Laurila, E.; Nieminen, H. J.; Peltonen, P.; Pokki, J.; Puisto, A.; Råback, P.; Salmenjoki, H.; Sironen, T.; Österberg, M. Modelling Aerosol Transport and Virus Exposure with Numerical Simulations in Relation to SARS-CoV-2 Transmission by Inhalation Indoors. *Saf. Sci.* **2020**, *130*, 104866.

(31) Chen, X.; Feng, Y.; Zhong, W.; Kleinstreuer, C. Numerical Investigation of the Interaction, Transport and Deposition of Multicomponent Droplets in a Simple Mouth-Throat Model. *J. Aerosol Sci.* **2017**, *105*, 108−127.

(32) Feng, Y.; Kleinstreuer, C.; Rostami, A. Evaporation and Condensation of Multicomponent Electronic Cigarette Droplets and Conventional Cigarette Smoke Particles in an Idealized G3-G6 Triple Bifurcating Unit. *J. Aerosol Sci.* **2015**, *80*, 58−74.

(33) Feng, Y.; Zhao, J.; Kleinstreuer, C.; Wang, Q.; Wang, J.; Wu, D. H.; Lin, J. An in Silico Inter-Subject Variability Study of Extra-Thoracic Morphology Effects on Inhaled Particle Transport and Deposition. *J. Aerosol Sci.* **2018**, *123*, 185−207.

(34) Haghnegahdar, A.; Zhao, J.; Feng, Y. Lung Aerosol Dynamics of Airborne Influenza A Virus-Laden Droplets and the Resultant Immune System Responses: An in Silico Study. *J. Aerosol Sci.* **2019**, *134*, 34−55.

https://doi.org/10.1021/acsomega.1c01489
ACS Omega 2021, 6, 16876−16889

(35) Zhao, J.; Feng, Y.; Bezerra, M.; Wang, J.; Sperry, T. Numerical Simulation of Welding Fume Lung Dosimetry. *J. Aerosol Sci.* **2019**, *135*, 113.
(36) Blocken, B.; Malizia, F.; Van Druenen, T.; Marchal, T. *Towards Aerodynamically Equivalent COVID19 1.5 m Social Distancing for Walking and Running*.
(37) Asadi, S.; Wexler, A. S.; Cappa, C. D.; Barreda, S.; Bouvier, N. M.; Ristenpart, W. D. Aerosol Emission and Superemission during Human Speech Increase with Voice Loudness. *Sci. Rep.* **2019**, *9*, 2348.
(38) Coronavirus disease (COVID-19): How is it transmitted? https://www.who.int/news-room/q-a-detail/coronavirus-disease-covid-19-how-is-it-transmitted (accessed May 12, 2021).
(39) Scientific Brief: SARS-CoV-2 Transmission | CDC https://www.cdc.gov/coronavirus/2019-ncov/science/science-briefs/sars-cov-2-transmission.html (accessed May 12, 2021).
(40) Lu, W.; Howarth, A. T. Numerical Analysis of Indoor Aerosol Particle Deposition and Distribution in Two-Zone Ventilation System. *Build. Environ.* **1996**, *31*, 41−50.
(41) KEYWORD COMMANDS. ANSWER® and CFDStudio®.
(42) Rajagopal, P. S.; Joshi, M.; Shinde, J.; Anand, S.; Runchal, A. K.; Sapra, B. K.; Mayya, Y. S.; Rao, M. M. Numerical Modeling of Aerosol Transport and Dynamics. *Energy for Propulsion* **2018**, 345−364.
(43) Rajagopal, P. S.; Magar, A.; Shinde, J.; Rao, M. M.; Runchal, A. K. CFD Simulation of Soot Dynamics in the Exhaust System of an Engine to Meet Particulate Standards of 2020 and Beyond. *Sustainable Development for Energy, Power, and Propulsion* **2021**, 463−479.
(44) Williams, M. M. R.; Loyalka, S. K. *Aerosol Science: Theory and Practice*. 1991.
(45) Prakash, A.; Bapat, A. P.; Zachariah, M. R. A Simple Numerical Algorithm and Software for Solution of Nucleation, Surface Growth, and Coagulation Problems. *Aerosol Sci. Technol.* **2003**, *37*, 892.
(46) Cunningham, E. On the Velocity of Steady Fall of Spherical Particles through Fluid Medium. *Proc. R. Soc. London. Ser. A, Contain. Pap. a Math. Phys. Character.* **1910**, *83*, 357−365.
(47) Guha, A. Transport and Deposition of Particles in Turbulent and Laminar Flow. *Annu. Rev. Fluid Mech.* **2008**, 311−341.
(48) Overholt, K. J.; Floyd, J. E.; Ezekoye, O. A. Computational Modeling and Validation of Aerosol Deposition in Ventilation Ducts. *Fire Technol.* **2016**, *52*, 149−166.
(49) Gregson, F. K. A.; Watson, N. A.; Orton, C. M.; Haddrell, A. E.; Mccarthy, L. P.; Finnie, T. J. R.; Gent, N.; Donaldson, G. C.; Shah, P. L. Comparing the Respirable Aerosol Concentrations and Particle Size Distributions Generated by Singing , Speaking and Breathing. *ChemRxiv* **2020**, *2*, 1−27.
(50) Gupta, J. K.; Lin, C. H.; Chen, Q. Characterizing Exhaled Airflow from Breathing and Talking. *Indoor Air* **2010**, *20*, 31−39.
(51) Morawska, L.; Johnson, G. R.; Ristovski, Z. D.; Hargreaves, M.; Mengersen, K.; Corbett, S.; Chao, C. Y. H.; Li, Y.; Katoshevski, D. Size Distribution and Sites of Origin of Droplets Expelled from the Human Respiratory Tract during Expiratory Activities. *J. Aerosol Sci.* **2009**, *40*, 256−269.
(52) Asadi, S.; Wexler, A. S.; Cappa, C. D.; Barreda, S.; Bouvier, N. M.; Ristenpart, W. D. Effect of Voicing and Articulation Manner on Aerosol Particle Emission during Human Speech. *PLoS One* **2020**, *15*, e0227699.
(53) Zhang, H.; Li, D.; Xie, L.; Xiao, Y. Documentary Research of Human Respiratory Droplet Characteristics. *Procedia Engineering* **2015**, *121*, 1365.
(54) Yu, K. P.; Lin, C. C.; Yang, S. C.; Zhao, P. Enhancement Effect of Relative Humidity on the Formation and Regional Respiratory Deposition of Secondary Organic Aerosol. *J. Hazard. Mater.* **2011**, *191*, 94−102.
(55) Nicas, M.; Nazaroff, W. W.; Hubbard, A. Toward Understanding the Risk of Secondary Airborne Infection: Emission of Respirable Pathogens. *J. Occup. Environ. Hyg.* **2005**, *2*, 143−154.
(56) Liu, L.; Wei, J.; Li, Y.; Ooi, A. Evaporation and Dispersion of Respiratory Droplets from Coughing. *Indoor Air* **2017**, *27*, 179−190.

https://doi.org/10.1021/acsomega.1c01489
ACS Omega 2021, 6, 16876−16889